Electronic Supplementary Material (ESI) for Physical Chemistry Chemical Physics.

Supplementary Information

Effects of a conductive support on the bonding of oxygen containing molecules to transition metal oxide surfaces

Hao Li and Jens K. Nørskov*

Catalysis Theory Center, Department of Physics, Technical University of Denmark,

2800 Lyngby, Denmark

***Corresponding Author:**

jkno@dtu.dk (J.K.N.);

Computational Methods

Density functional theory (DFT) calculations were performed using the generalized gradient approximation (GGA) method with the revised Perdew−Burke−Ernzerhof (RPBE) functional to describe electronic exchange and correlations.[1,2] A projector augmented-wave method was used to describe the core electrons.[3] Valence electrons were described by expanding the Kohn-Sham wave functions in a plane-wave basis set,[4] with the cutoff of 400 eV. Convergence was defined when all the forces were lower than 0.05 eV/Å. Bader charge analysis was performed to analyze the electron charges.[5] (3×3×1), (3×3×1), (3×3×1), (1×3×1), and (1×1×1) *k*-point meshes were used to sample the Brillouin zone using the Monkhorst-Pack method,[6] respectively for PdO_2(110), SnO_2(110), ZrO_2(100), HfO_2(111), and the thick supported ZrO_2(100) systems. A dipole correction was applied to the *z*-direction of each surface. Stricter criteria were tested for all of the transition metal oxide (TMO) systems; no significant difference was found in the adsorption configuration and binding energy. The bulk TMO structures were obtained from the *MaterialsProject* database.[7] Bulk optimizations were performed for each TMO system before their surfaces were cleaved. The optimized structures of the surfaces are shown in **Figure S1**. For each system shown in **Figure S1**, the bottom half of the slab was constrained, while the topmost layers were allowed to relax. For the supported ZrO_2(100) systems considered for the thickness-dependent study, the topmost three layers were allowed to relax, while the rest of the layers were constrained. Single-point energy calculations with a hybrid functional (HSE06)[8] were performed for both ZrO_2(100) and ZrO_2(100)/Au; no significant difference was found in the electron charge information compared to the results from RPBE (**Figure S9**). Surface Pourbaix diagrams were

calculated using the method described by Ref.[9], with pH=0. The binding energies were calculated using the total energies of H_2 and H_2O as the references:

$$E_{O*} = E_{tot} - E_{bare} - E_{H_2O} + E_{H_2}, \quad (1)$$

$$E_{HO*} = E_{tot} - E_{bare} - E_{H_2O} + \frac{1}{2}E_{H_2}, \quad (2)$$

$$E_{HOO*} = E_{tot} - E_{bare} - 2E_{H_2O} + \frac{3}{2}E_{H_2}, \quad (3)$$

where E_{tot} is the total energy of the surface with adsorbate, E_{bare} is the total energy of a bare surface, E_{H_2O} is the total energy of a H_2O molecule in vacuum, and E_{H_2} is the total energy of a H_2 molecule in vacuum.

References

1 J. P. Perdew, K. Burke and M. Ernzerhof, Generalized Gradient Approximation Made Simple, *Phys. Rev. Lett.*, 1996, **77**, 3865–3868.

2 B. Hammer, L. B. Hansen and J. K. Nørskov, Improved adsorption energetics within density-functional theory using revised Perdew-Burke-Ernzerhof functionals, *Phys. Rev. B - Condens. Matter Mater. Phys.*, 1999, **59**, 7413.

3 P. E. Blöchl, Projector augmented-wave method, *Phys. Rev. B*, 1994, **50**, 17953–17979.

4 W. Kohn and L. J. Sham, Self-consistent equations including exchange and correlation effects, *Phys. Rev.*, 1965, **140**, A1133.

5 W. Tang, E. Sanville and G. Henkelman, A grid-based Bader analysis algorithm without lattice bias, *J. Phys. Condens. Matter*, 2009, **21**, 084204.

6 H. Monkhorst and J. Pack, Special points for Brillouin zone integrations, *Phys. Rev. B*, 1976, **13**, 5188–5192.

7 A. Jain, S. P. Ong, G. Hautier, W. Chen, W. D. Richards, S. Dacek, S. Cholia, D. Gunter, D. Skinner, G. Ceder and K. A. Persson, *APL Mater.*, 2013, 011002.

8 A. V. Krukau, O. A. Vydrov, A. F. Izmaylov and G. E. Scuseria, Influence of the exchange screening parameter on the performance of screened hybrid functionals, *J. Chem. Phys.*, 2006, **125**, 224106.

9 H. A. Hansen, J. Rossmeisl and J. K. Nørskov, Surface Pourbaix diagrams and oxygen reduction activity of Pt, Ag and Ni(111) surfaces studied by DFT, *Phys. Chem. Chem. Phys.*, 2008, **10**, 3722–3730.

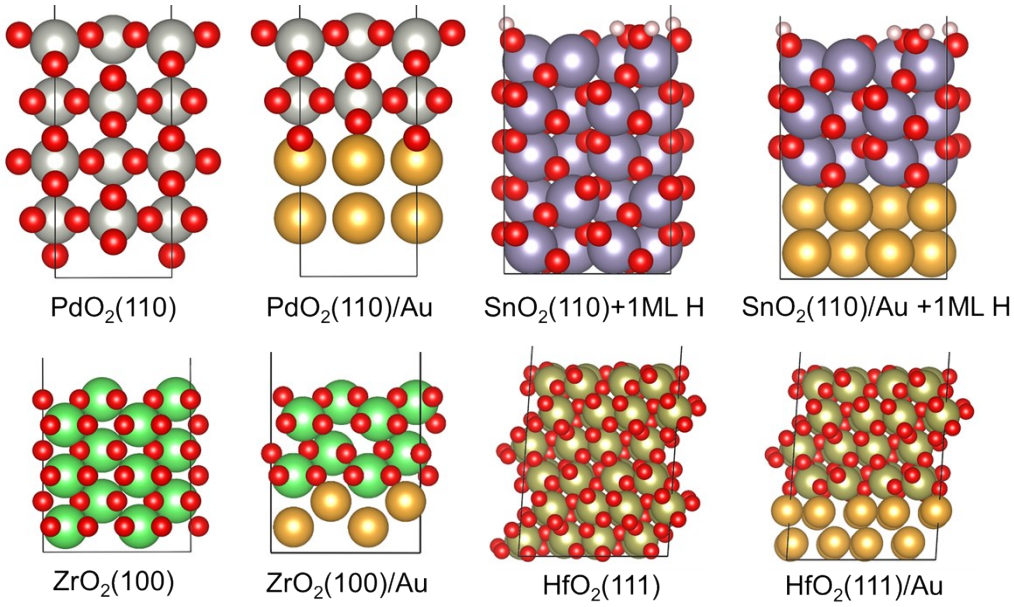

Figure S1. TMO and Au-supported TMO structures considered for the binding energy calculations in **Table 1**. Red, pink, gold, grey, purple, green, and brown spheres represent O, H, Au, Pd, Sn, Zr, and Hf, respectively. More information of the Au substrate are shown in **Table S3**.

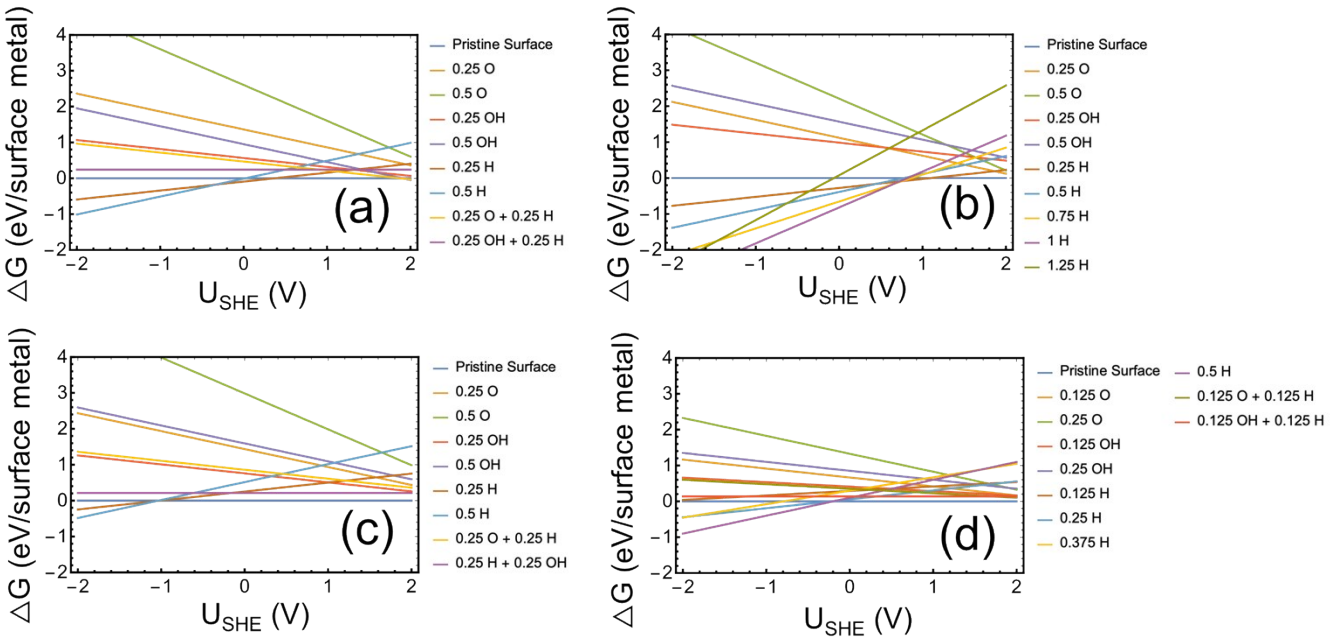

Figure S2. Calculated surface Pourbaix diagrams for (a) PdO_2(110), (b) SnO_2(110), (c) ZrO_2(100), and (d) HfO_2(111). The pristine surfaces are shown in **Figure S1**.

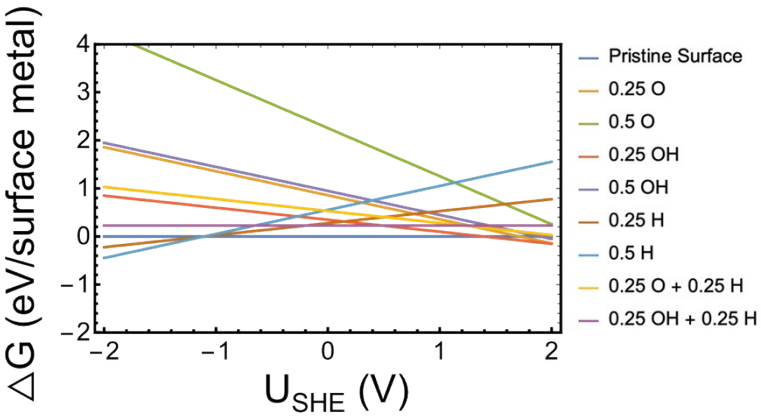

Figure S3. Calculated surface Pourbaix diagram for 4L ZrO_2(100)/Au. The pristine surface structure is shown in **Figure 1b**.

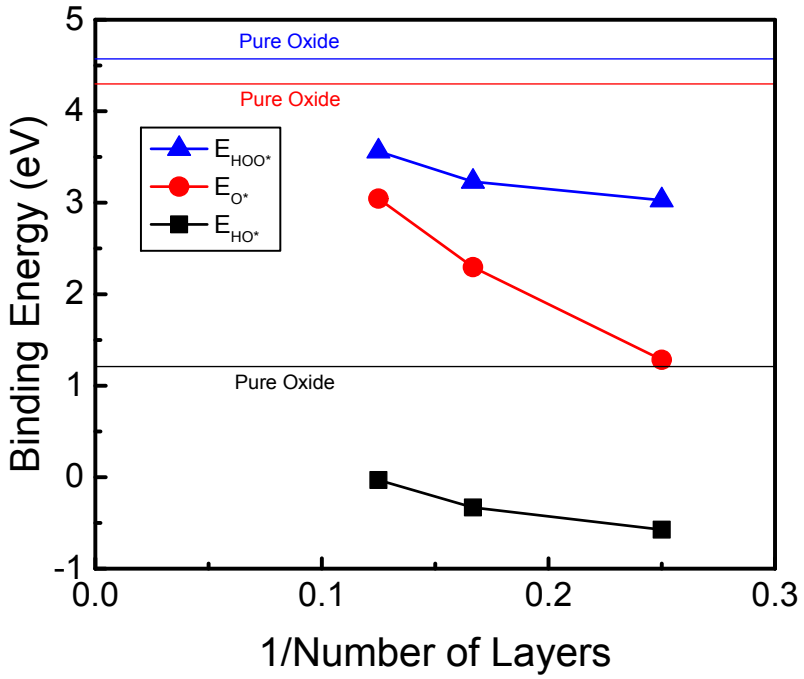

Figure S4. Calculated binding energies of ORR/OER adsorbate on larger ZrO_2(100)/Au surfaces with varying oxide thickness. These calculations are with the unit cell twice size of those in **Figure 1**. The horizontal lines represent the adsorbate binding energies calculated on pure ZrO_2(100).

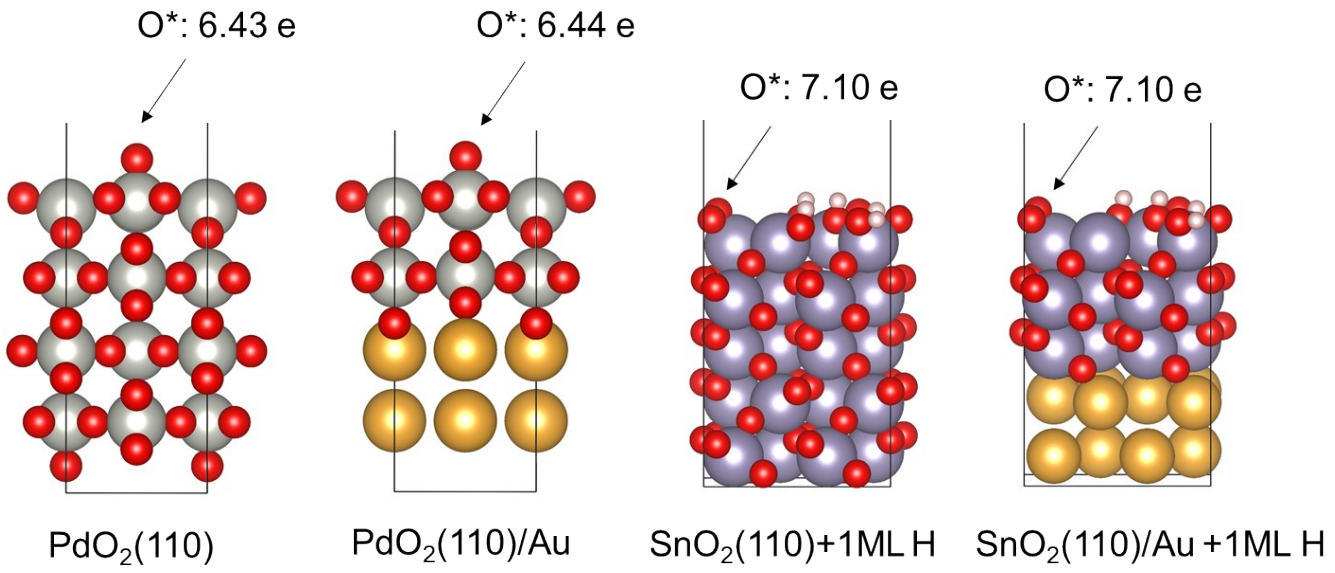

Figure S5. Calculated electron charge of adsorbed O* at the metal-like TMO structures. Red, pink, gold, grey, and purple spheres represent O, H, Au, Pd, and Sn, respectively.

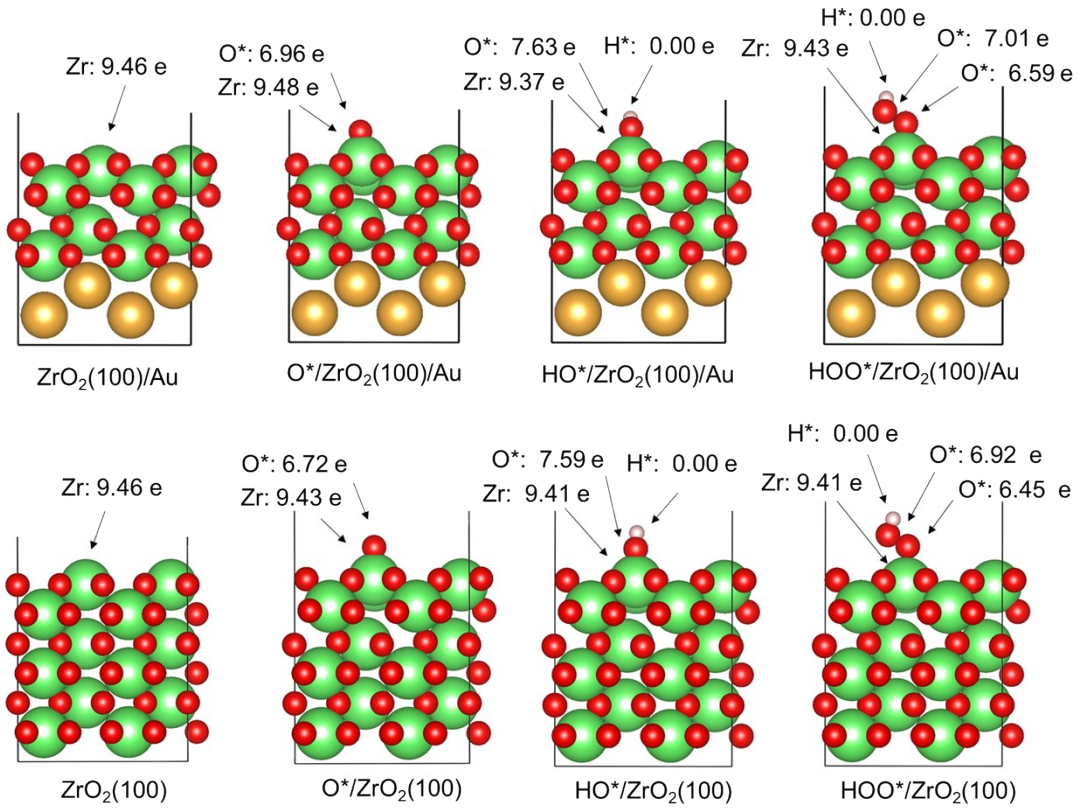

Figure S6. Calculated electron charges of $ZrO_2(100)$/Au, O*/$ZrO_2(100)$/Au, HO*/$ZrO_2(100)$/Au, HOO*/$ZrO_2(100)$/Au, $ZrO_2(100)$, O*/$ZrO_2(100)$, HO*/$ZrO_2(100)$, and HOO*/$ZrO_2(100)$ by Bader charge analysis. Red, gold, green, and pink spheres represent O, Au, Zr, and H, respectively.

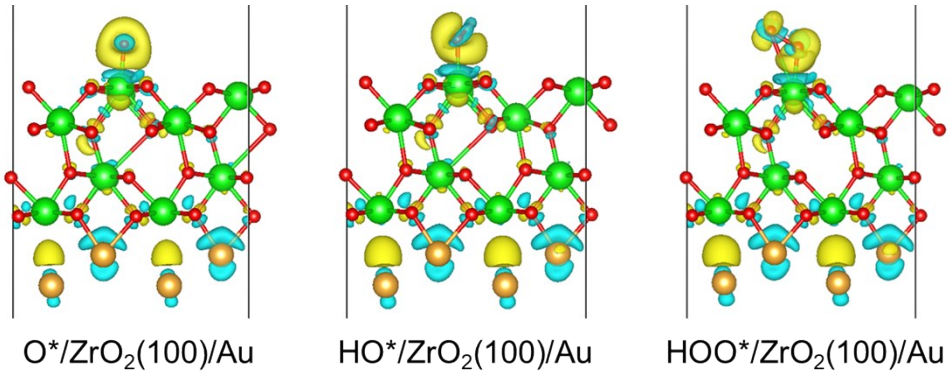

Figure S7. Calculated charge density differences of ZrO_2(100)/Au with adsorbed ORR/OER adsorbate. Red, pink, gold, and green spheres represent O, H, Au, and Zr, respectively. The yellow and teal colors in the isosurfaces represent electron charge gain and loss, respectively. The charge density difference was calculated by $\Delta\rho = \rho_1 - \rho_2 - \rho_3 - \rho_4$ (where ρ_1, ρ_2, ρ_3, and ρ_4 represent the charge densities of the whole system, the oxide layer, Au-support, and the adsorbate, respectively).

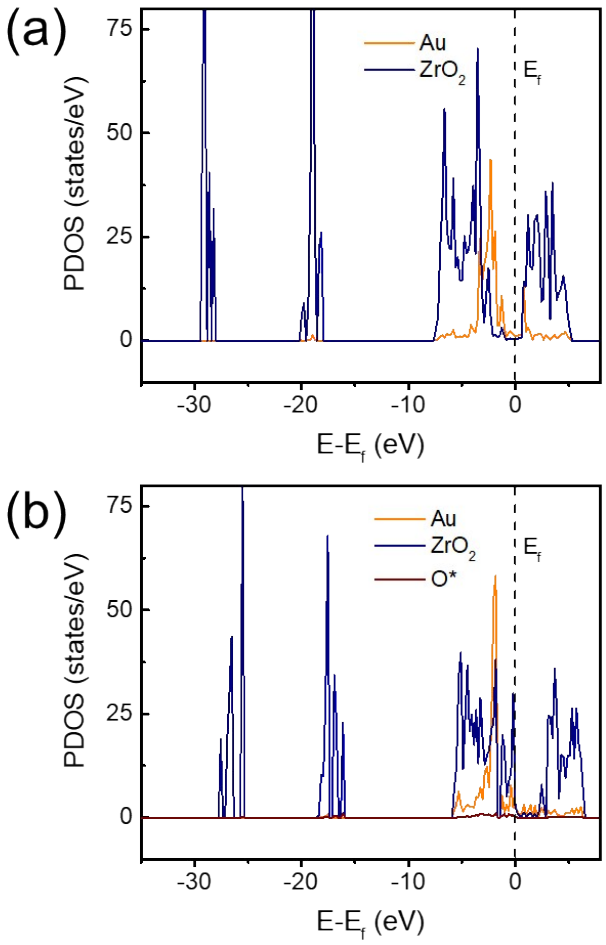

Figure S8. Calculated projected density of states of (a) ZrO_2(100)/Au and (b) O*/ZrO_2(100)/Au. The black dashed line represents the Fermi level (E_f).

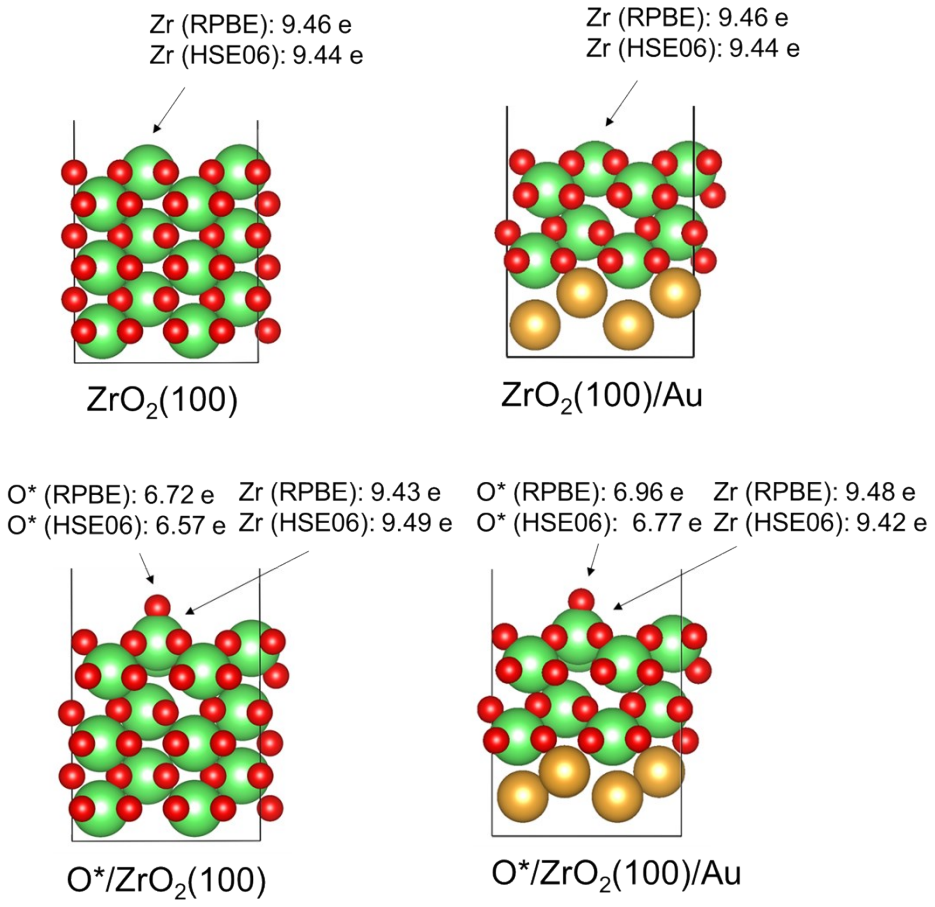

Figure S9. Comparison between the RPBE and HSE06 functionals on the calculated electron charge information of $ZrO_2(100)$ and $ZrO_2(100)$/Au. Red, gold, and green spheres represent O, Au, and Zr, respectively.

Table S1. Calculated ORR/OER adsorbate binding energies on $ZrO_2(100)$ and $ZrO_2(100)/Zr$.

Catalyst	**E_{HO*} (eV)**	**E_{O*} (eV)**	**E_{HOO*} (eV)**
$ZrO_2(100)$	1.42	4.58	4.62
$ZrO_2(100)/Au$	-0.22	2.27	3.40
ΔE	-1.64	-2.31	-1.22
$ZrO_2(100)/Zr$	-0.78	1.05	2.79
ΔE	-2.20	-3.55	-1.83

Table S2. Calculated ORR/OER adsorbate binding energies on wide-bandgap TMOs with varying thickness.

Catalyst	**E_{HO*} (eV)**	**E_{O*} (eV)**	**E_{HOO*} (eV)**
20L ZrO_2(100)	1.57	4.59	4.85
18L ZrO_2(100)	1.39	4.54	4.64
16L ZrO_2(100)	1.40	4.56	4.65
14L ZrO_2(100)	1.41	4.57	4.65
12L ZrO_2(100)	1.40	4.54	4.65
10L ZrO_2(100)	1.42	4.53	4.64
8L ZrO_2(100)	1.36	4.52	4.63
6L ZrO_2(100)	1.42	4.58	4.62
4L ZrO_2(100)	1.54	4.71	4.73
6L HfO_2(111)	1.68	3.67	4.77
4L HfO_2(111)	1.62	3.00	4.73

Table S3. Distance of Au-M (where M is the nearest cation) in the Au-support along the *x*-, *y*-, and *z*-directions.

Model	***x* (Å)**	***y* (Å)**	***z* (Å)**
PdO_2(110)/Au	3.18	3.59	3.59
SnO_2(110)/Au	4.86	3.78	3.78
ZrO_2(100)/Au	3.64	5.28	3.46
HfO_2(111)/Au	3.95	4.07	3.33